Dynamic scaling approach to glass formation

Ralph H. Colby
Materials Science and Engineering, The Pennsylvania State University, University Park, Pennsylvania 16802
(Received 4 June 1999)

Experimental data for the temperature dependence of relaxation times are used to argue that the dynamic scaling form, with relaxation time diverging at the critical temperature T_c as $(T-T_c)^{-\nu z}$, is superior to the classical Vogel form. This observation leads us to propose that glass formation can be described by a simple mean-field limit of a phase transition. The order parameter is the fraction of all space that has sufficient free volume to allow substantial motion, and grows logarithmically above T_c. Diffusion of this free volume creates random walk clusters that have cooperatively rearranged. We show that the distribution of cooperatively moving clusters must have a Fisher exponent $\tau=2$. Dynamic scaling predicts a power law for the relaxation modulus $G(t)\sim t^{-2/z}$, where z is the dynamic critical exponent relating the relaxation time of a cluster to its size. Andrade creep, universally observed for all glass-forming materials, suggests $z=6$. Experimental data on the temperature dependence of viscosity and relaxation time of glass-forming liquids suggest that the exponent ν describing the correlation length divergence in this simple scaling picture is not always universal. Polymers appear to *universally* have $\nu z=9$ (making $\nu=\frac{3}{2}$). However, other glass-formers have unphysically large values of νz, suggesting that the availability of free volume is a necessary, but not sufficient, condition for motion in these liquids. Such considerations lead us to assert that $\nu z=9$ is in fact universal for all glass-forming liquids, but an energetic barrier to motion must also be overcome for strong glasses.

PACS number(s): 64.70.Pf, 61.43.Fs, 83.50.Fc

I. INTRODUCTION

Many materials form amorphous glasses on cooling from the liquid state [1–4], in lieu of crystallizing. Examples include common silica window glass, many ''floppy'' organic small molecules, such as 1,2-diphenyl benzene, and many polymers. Despite the fact that the structure of the amorphous glass is essentially identical to a ''snapshot'' of the liquid state, a detailed understanding of glass formation has eluded physicists for many years. In this paper, we explore the utility of the modern critical phenomena description of phase transitions [5] for understanding glass formation. Such an approach has been suggested based on computer simulations of simple glass-forming liquids [6] and polymers [7], and has seen some successes in recent years [8,9].

Underlying glass formation is a constrained motion problem. In 1965 Adam and Gibbs [10] suggested that, near the operationally defined glass transition temperature T_g, motion is *highly* cooperative. Some regions of the sample have to wait for their immediate neighbors to move before they can move, owing to the density being too large for liquidlike motion. Using this simple idea in the framework of dynamic scaling for continuous phase transitions [5,11], we write that the relaxation time $\mathcal{T}$ and size ξ of these cooperatively rearranging regions diverge at a critical temperature T_c, with the form

$$\mathcal{T}\sim\xi^z\sim\varepsilon^{-\nu z}, \tag{1}$$

where z is the dynamic exponent, ε is the proximity to the critical point

$$\varepsilon\equiv(T-T_c)/T_c \tag{2}$$

and the exponent ν describes the divergence of the correlation length ξ

$$\xi\sim\varepsilon^{-\nu}. \tag{3}$$

Figure 1 shows an application of Eq. (1) to experimental data for polyvinyl-methylether (PVME), a glass-forming polymer with $T_g=-24\,^\circ$C. Two sets of data, from oscillatory shear [12,13] (OS, circles) and dielectric spectroscopy [12] (DS, squares) experiments are shown, using the *same critical temperature* $T_c=-40\,^\circ\text{C}=T_g-16$ K. These data show that Eq. (1) describes the temperature dependence of relaxation processes reasonably. The same data are also described reasonably by the empirical Vogel relation [14,15]

$$\mathcal{T}\sim\exp[B(T-T_g)/(T-T_\infty)], \tag{4}$$

where B is a constant and T_∞ is the Vogel temperature. However, unlike the scaling form of Eq. (1), the temperature where the relaxation times diverge in the Vogel form is different for the two experiments ($T_\infty=-94\,^\circ\text{C}=T_g-70$ K for OS and $T_\infty=-69\,^\circ\text{C}=T_g-45$ K for DS) [12], strongly suggesting that the Vogel relation is of the wrong form, with similar results observed for other polymer glass-formers [16–22]. The fact that the same critical temperature T_c describes both sets of data in Fig. 1 is strong evidence that Eq. (1) may have some physical significance.

Furthermore, viscoelastic data on another polymer, atactic polymethyl-methacrylate (PMMA, with $T_g=106\,^\circ$C) are known to not be described adequately by the Vogel relation [23] [Eq. (4)] but are described within the precision of the measurements by Eq. (1) with $T_c=97\,^\circ\text{C}=T_g-9$ K (shown as the triangles in Fig. 1). The fact that the critical temperature is only roughly 10 K below the operational glass transition makes the dynamic scaling approach more intuitive than the Vogel relation, for which the relaxation time diverges at T_∞, roughly 50 K below T_g for most glass-forming polymers [24]. Adam and Gibbs [10] gave some physical interpretation

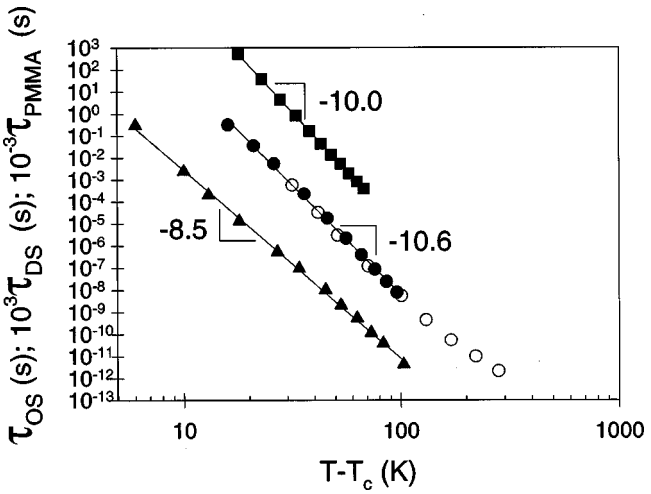

FIG. 1. Critical scaling for the temperature dependence of segmental relaxation times for PVME using a critical temperature $T_c = -40\,^{\circ}\mathrm{C}$ and for atactic PMMA using a critical temperature $T_c = 97\,^{\circ}\mathrm{C}$. Circles are the reciprocal of the frequency at which the glassy loss modulus of PVME has a maximum in oscillatory shear [filled (Ref. [12]), open (Ref. [13])], using time-temperature superposition. Squares are the relaxation time from dielectric spectroscopy (multiplied by 1000 for clarity) as determined by fitting data to the Havriliak-Negami function [described elsewhere (Ref. [12])]. Triangles are the segmental relaxation time from creep on atactic PMMA (Ref. [23]).

of T_∞ as the temperature at which the configurational entropy is zero, but a recent simulation finds that some configurational entropy remains [25] even below T_∞.

Mode coupling theory [26] uses the same form as Eq. (1) to describe the high-temperature relaxation time data, but use T_c that is 30–70 K *above* T_g. As a result, they find considerably smaller values of the exponent νz, and also need to splice on an empirical form such as Eq. (4) to describe the relaxation time between T_g and T_c.

II. SCALING MODEL

Since the scaling form of Eq. (1) appears promising, we are motivated to understand the physics behind it, with regard to glass formation. We thus construct a simple mean-field model, based on the idea of cooperative motion introduced by Adam and Gibbs [10]. Glass-forming liquids near T_g are *dynamically heterogeneous*: only some small fraction of the material is able to move at a given point in time [27]. We define a ⟨⟨particle⟩⟩ as the smallest entity capable of random motion. The particle of a flexible polymer is of order the monomer size, while for silica it is presumably a single Si atom. We define ⟨⟨motion⟩⟩ to occur when a particle moves a distance of order of its own size. There is a broad distribution of free volume sizes in any amorphous material. [28,29] In the glassy state, the distribution is cutoff below the critical size that allows for particle motion. The particles are confined to the ⟨⟨cage⟩⟩ made up of surrounding particles and large-scale motion is not allowed. In contrast, the liquid state always has some part of the free volume distribution that exceeds the critical free-volume size for motion. Near the glass transition, patches of free volume larger than the critical size are rare, but as the material is heated such

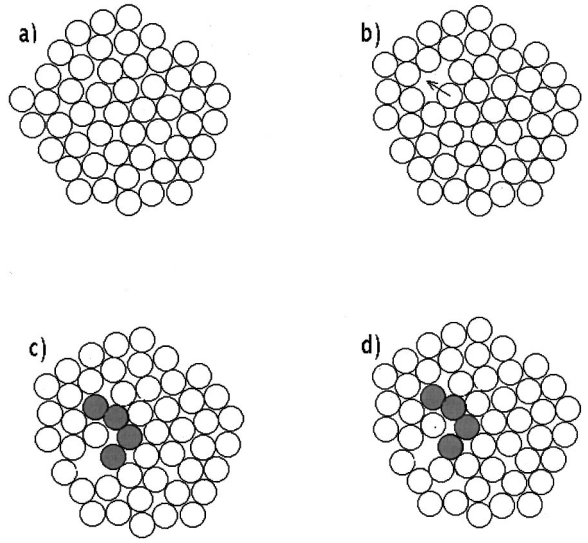

FIG. 2. 2-*d* representation of particles in a liquid near T_g. (a) Particles unable to move—initially particles can only vibrate in their cages of surrounding particles because there is no free volume of sufficient size for particle motion on distances of order of the particle size in this region. (b) Critical free volume forms—random motion of particles in their cages results in a single free volume of sufficient size for particles to move. The arrow denotes the particle that is about to exchange places with the free volume. (c) Free volume diffusion—a random-walk chain of particles that have moved by exchanging places with the free volume is shown as the shaded particles. (d) Critical free volume disperses—the free volume disperses by splitting into free volumes that are too small for particle motion on length scales comparable to the particle size.

patches become more prevalent, since the density decreases as temperature is raised. These considerations lead to a natural definition for the *order parameter*: the fraction of the material that has sufficient free volume for particle motion. Below T_c the order parameter is zero, while above T_c it slowly grows as the temperature is raised. We next present a simple scaling model that predicts such a slow (logarithmic) growth of the order parameter.

Above T_c, but near the glass transition, there are only isolated patches of sufficient free volume for particle motion. Creation of such a free volume is shown in Figs. 2(a) and 2(b). The free volume that exceeds the critical size for motion diffuses randomly until the point in time where it disperses by splitting into smaller pieces of free volume that are no longer large enough for motion, as shown in Figs. 2(c) and 2(d). We define a ⟨⟨cluster⟩⟩ as the particles that were visited (and hence moved) by the free volume during its random walk before it disperses [the shaded particles in Figs. 2(c) and 2(d)]. Thus, each cluster is a random walk of particles that have cooperatively rearranged, in that they all used the same free volume to move. This physical picture is consistent with, and very much inspired by, recent simulation results [30] which find stringlike cooperative motion in glass-forming liquids near T_g. The picture in Fig. 2 is a greatly oversimplified view of cluster formation. Many other particle motions are possible, such as the cooperative rotation of n particles that roughly form a larger sphere. The details of these motions depend on the specific glass-forming material considered. Indeed, even the simple Lennard-Jones

sphere mixtures used for molecular dynamics simulations often exhibit more complex clusters than simple linear-chain random walks (although pictures quite similar to Fig. 2 are often observed [30]). However, there is a *universal aspect shared by all clusters of cooperatively rearranged particles*: The clusters are always formed by a random walk of the free volume through the material, making the cluster's *fractal dimension* $D=2$.

Recent simulations report no thermodynamic divergences as temperature is lowered [25] (even below T_∞), suggesting the utility of a percolation model, as this class of models is known to have no thermodynamic divergences. In any finite time interval, free volume of the critical size will randomly form, diffuse and disperse, leaving a distribution of random-walk clusters of varying sizes. Since both creation and destruction of free volume exceeding the critical size are random processes, with no particular length scale, there should be a power law distribution of cluster sizes, cut off by a largest size that diverges at the critical point. As the liquid is cooled (i.e., as T_c is approached from above) the order parameter decreases. Motion is still possible for every particle, but the entire process takes much longer, allowing progressively larger clusters to be created.

The distribution function $P(n)$ for the number n of particles in a cluster has the form [31]

$$P(n)\sim n^{-\tau}(-n/S), \tag{5}$$

where τ is the Fisher exponent describing that power-law distribution, and

$$S\sim \varepsilon^{-1/\sigma}, \tag{6}$$

is the number of particles in the largest cooperatively rearranging clusters [whose size defines the correlation length ξ of Eqs. (1) and (3)]. The self-correlation function $g(r)$ of each cluster is of the Ornstein-Zernike form [5] since each cluster is a random walk

$$g(r)\sim \frac{\exp(-r/\xi)}{r}. \tag{7}$$

The average cluster size in the distribution $\overline{S}$ also diverges at the critical point

$$\overline{S}\sim \varepsilon^{-\gamma}, \tag{8}$$

and can be determined by summing all self-correlation functions [31]

$$\overline{S}\sim \sum g(r)\sim \xi^3 g(\xi)\sim \xi^2, \tag{9}$$

meaning that the exponents are related as

$$\gamma=2\nu. \tag{10}$$

The size and mass of the largest cluster are related by the fractal dimension [31] D, as

$$S\sim \xi^D, \tag{11}$$

which requires

$$\frac{1}{\sigma}=D\nu. \tag{12}$$

Combining these with the scaling relation $\gamma=(3-\tau)/\sigma$, leads to a general result for mean field [32]

$$\frac{2}{D}=3-\tau, \tag{13}$$

which we note is obeyed for mean-field percolation [31] as well (where $D=4$ and $\tau=5/2$). Since free volume diffuses randomly, each cluster is a random walk, so $D=2$, making $\tau=2$. The exponent for the order parameter is then zero [$\beta=(\tau-2)/\sigma=0$]. The universality class with $\tau=2$ has $\beta=0$, consistent with the slowly growing order parameter defined above. The glass transition is analogous to 1-*d* percolation [31], in that the solid phase side of the transition ($T<T_c$) has no static distinction. As T_c is approached from above, the cooperatively rearranging clusters get larger, and for $T\leqslant T_c$ the entire sample must move cooperatively, effectively prohibiting particles from moving any distance of order of their own size. In summary, the glass transition has

$$\tau=2 \quad D=2 \quad \beta=0, \tag{14}$$

with the following relations between exponents:

$$2\nu=\gamma=1/\sigma. \tag{15}$$

Recent molecular dynamics simulations of Lennard-Jones sphere mixtures [33–35] suggest that Eq. (5) with $\tau=2$ is indeed the correct description of the cooperatively moving cluster distribution. They determined the distribution function of clusters $P(n)$, normalized such that $P(1)=1$. With this normalization and $\tau=2$, Eq. (5) is rewritten as

$$n^2P(n)=\exp\left(\frac{1-n}{S}\right). \tag{16}$$

By plotting $\ln[n^2P(n)]$ against n, we determined S for each of the seven temperatures they studied. We then use the S values to construct the scaling curve shown in Fig. 3. The solid curve in Fig. 3 is Eq. (16). Figure 3 is strong evidence that Eq. (5) with $\tau=2$ is a reasonable form for the cluster distribution function. Owing to the rather limited temperature range covered in the simulations, we did not attempt to determine other exponents.

The measured quantities of interest here are the relaxation times shown in Fig. 1, motivating us to consider dynamic scaling. We make the standard dynamic scaling assumption [11], that each cluster of n particles has a size r_n that determines its relaxation time $\mathcal{T}_n$,

$$\mathcal{T}_n\sim r_n^z\sim n^{z/D}. \tag{17}$$

The stress relaxation modulus [24] $G(t)$ is calculated from the distribution of cluster sizes, assuming linear additivity

$$G(t)=\int_0^\infty P(n)\exp(-t/\mathcal{T}_n)dn\sim t^{-D(\tau-1)/z}. \tag{18}$$

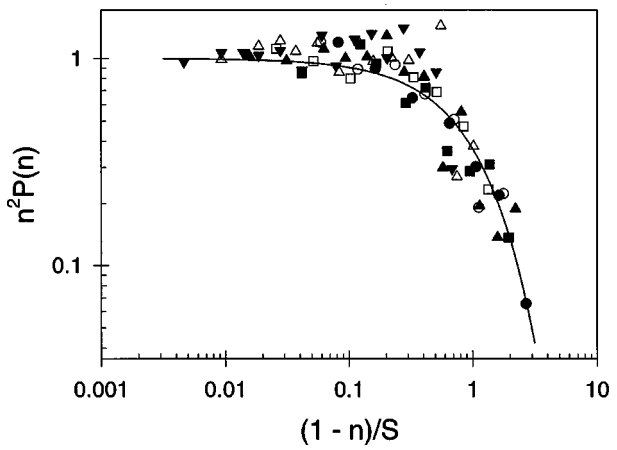

FIG. 3. Cluster distribution function from the molecular dynamics simulations of Lennard-Jones liquids by Donati *et al.* (Ref. [34]) in the scaling form of Eq. (5) with $\tau=2$. Reduced temperatures k_BT/ε [where ε is the principle interparticle interaction energy (Ref. [35])] are 0.5495 (filled circles), 0.5254 (open circles), 0.5052 (filled squares), 0.4795 (open squares), 0.4685 (filled triangles), 0.4572 (open triangles), and 0.4510 (inverted triangles).

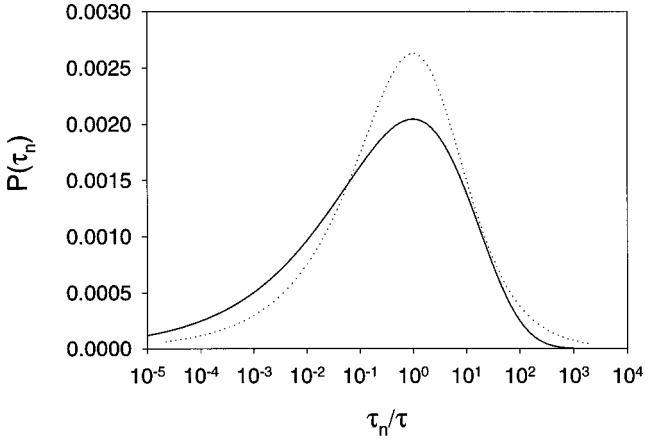

FIG. 4. Comparison of the distribution of segmental relaxation times predicted by the scaling model [Eq. (21), solid curve] and those measured by dielectric spectroscopy for PVME (dotted curve). The experimental curve was calculated from the empirical Havriliak-Negami function (Ref. [41]) which fit the experimental dielectric data very well (Ref. [12]).

For glass formation, $D=2$ and $\tau=2$, so dynamic scaling predicts

$$G(t)\sim t^{-2/z}. \tag{19}$$

Note that for 3-*d* critical percolation [31] $D=2.5$, $\tau=2.2$ and the experimental dynamic exponent [36] $z=4.5$, making the exponent in Eq. (18) $-D(\tau-1)/z=-0.67$, in good agreement with the experimentally observed [37] $G(t)\sim t^{-0.66}$ for randomly branched polymers in the critical percolation class.

For glass-forming materials, recoverable creep compliance data universally show the Andrade result [38–40]: $J(t)\sim t^{1/3}$ near T_g. This is demonstrated beautifully in Fig. 3.50 of the Dissertation by Bero [40], where the retardation spectra of fourteen different glass-forming liquids are compared with their glass transition as the reference temperature. They all show $J(t)\sim t^{1/3}$ in the same range: $10^{-13}<J<10^{-10}\,\mathrm{cm^2/dyne}$ and $10^{-5}<t<10^{5}\,\mathrm{s}$. For a power law, $J(t)\sim 1/G(t)$, making $z=6$ from creep and recovery experiments on glass-forming liquids.

The entire relaxation time distribution can be calculated from the cluster distribution function [Eq. (5)] and the dynamic scaling assumption [Eq. (17)]. The distribution of relaxation times

$$P(\mathcal{T}_n)d\mathcal{T}_n\sim\frac{d\mathcal{T}_n}{dn}nP(n)dn\sim\mathcal{T}_n^{1-\tau D/z}\exp(-\mathcal{T}_n^{D/z}/S)d\mathcal{T}_n$$
$$\sim\mathcal{T}_n^{1-\tau D/z}\exp\left[-\left(\frac{\mathcal{T}_n}{\mathcal{T}}\right)^{D/z}\right]d\mathcal{T}_n, \tag{20}$$

is the product of a power law and a stretched exponential cutoff, where the final relation was obtained by applying the dynamic scaling assumption to the largest cluster ($\mathcal{T}\sim S^{z/D}$). For glass-forming liquids, $D=2$, $\tau=2$ and $z=6$, making

$$P(\mathcal{T}_n)d\mathcal{T}_n\sim\mathcal{T}_n^{1/3}\exp\left[-\left(\frac{\mathcal{T}_n}{\mathcal{T}}\right)^{1/3}\right]d\mathcal{T}_n. \tag{21}$$

Hence, our simple scaling model predicts the form of the distribution of relaxation times with no adjustable parameters. We compare this distribution with the experimental segmental relaxation time distribution of PVME calculated from dielectric spectroscopy data [12] using the Havriliak-Negami function [41] in Fig. 4. While the agreement is not quantitative, the overall shape of the distribution of relaxation times is quite well described by the scaling model.

III. COMPARISON WITH EXPERIMENT

A formal theory for both ν and z is still needed to complete our understanding of glass formation. Unfortunately, experiments indicate that ν may be nonuniversal. This may mean that there are multiple universality classes, or it could mean there is no universal description. The latter is the currently favored view, and Angell has proposed a scheme for classifying glass-formers based on the proximity of their Vogel temperature to their glass transition [3] (T_g-T_∞). Inspired by this, we now investigate whether the observed exponents are correlated by the appropriate ''fragility'' parameter from our dynamic scaling model (T_g-T_c). The results of analyzing data similar to the data of Fig. 1 for a variety of glass-forming materials are summarized in Table I and Fig. 5. We determine νz and T_c by minimizing the sum of the squares of the residuals in log τ (or log η, when viscosity data are used [42]) fit to Eq. (1). A different procedure used by Souletie [8] leads to consistently larger values of νz and smaller values of T_c. Note that with our method, independent determinations of νz and T_c for the same material result in excellent agreement in most cases (see the multiple entries for salol, ortho-terphenyl, cis-PI, PVA*c*, PVME, PVE, atactic-PP and propylene carbonate in Table I. To determine the error bars in Fig. 5, we try various T_c around the optimal one, and do not allow the correlation coefficient r^2 to be less than 0.999 times its optimum value.

TABLE I. Exponents and critical temperatures for glass-forming liquids fit to Eq. (1) with $z=6$.

Material	Method	T_g (°C)	T_c (°C)	T_g-T_c (K)	νz	ν
SiO_2	viscosity [46,48]	1173	650±150	520	20.3±6	3.4±1
GeO_2	viscosity [46]	545	360±50	185	12.3±1	2.1±0.2
B_2O_3	viscosity [49]	275	100±90	175	28±10	4.7±2
$Pd_{48}N_{32}P_{20}$	kinetics [50]	292	217±30	75	14.7±4	2.5±0.7
$Pt_{45}Ni_{30}P_{25}$	kinetics [50]	209	137±30	72	15.6±5	2.6±0.8
salol	viscosity [51]	−60	−131±50	71	52±30	8.7±5
salol	DS [52,53]	−53	−84±15	31	24±8	4.0±1
Aroclor 1248	creep [43]	−50	−120±30	70	45±20	7.5±3
α-phenyl-*o*-cresol	viscosity [51]	−63	−133±50	70	54±30	9.0±5
6-phenyl ether	creep [43]	−25	−80±30	55	41±20	6.8±3
$Pd_{77.5}Cu_6Si_{16.5}$	kinetics [50]	340	307±10	33	10.5±2	1.8±0.4
ortho-terphenyl	DS [52,54]	−29	−62±10	33	24±7	4.0±1
ortho-terphenyl	creep [43]	−32	−65±15	33	27±10	4.5±2
ortho-terphenyl	viscosity [51]	−33	−65±20	32	28±10	4.7±2
kresolphtalein-dimethylether	DS [52,55]	38	8±10	30	19±3	3.2±0.5
phenolphtalein-dimethylether	DS [52,55]	21	−6±10	27	19±5	3.2±0.8
cis-polyisoprene (cis-PI)	OS [22]	−63	−90±11	27	21±10	3.5±2
cis-PI (segmental)	DS [22]	−63	−88±9	25	19±5	3.2±1
polyvinylacetate (PVA*c*)	creep [56,57]	35	27±2	8	9.8±1	1.6±0.2
PVA*c* (segmental)	DS [52]	30	10±5	20	12±2	2.0±0.3
1-propanol	DS [52,54]	−168	−185±6	17	11.9±2	2.0±0.3
PVME	OS [12]	−24	−42±5	18	10.5±1	1.8±0.2
PVME (segmental)	DS [12]	−24	−39±6	15	10.3±2	1.7±0.4
Selenium	viscosity [58,59]	27	10±3	17	11.5±1	1.9±0.2
polyvinylethylene (PVE)	DS [60]	0	−14±5	14	10.8±3	1.8±0.5
PVE	DS [61]	0	−13±8	13	10.5±3	1.8±0.5
1,4-PI (segmental)	DS [60]	−63	−74±4	11	9.6±2	1.6±0.4
glycerol	DS [62]	−93	−103±5	10	13.5±2	2.3±0.4
atactic polypropylene (PP)	creep [63]	−14	−24±5	10	9.7±2	1.6±0.4
atactic PP (segmental)	LS,OS,creep [21]	−14	−23±2	9	14.6±2	2.4±0.4
propylene carbonate	viscosity [64]	−119	−128±5	9	16.3±4	2.7±0.7
propylene carbonate	DS [52,53]	−116	−122±3	6	11.5±2	1.9±0.3
atactic (PMMA)	creep [23]	106	97±2	9	8.5±1	1.4±0.2
1,4-polybutadiene (PB)	OS [65]	−99	−103±3	4	8.6±1	1.4±0.2
2-methyltetrahydrofuran	DS [52,66]	−182	−184±2	2	11.2±2	1.9±0.3
$[KNO_3]_{60}[Ca(NO_3)_2]_{40}$	viscosity [67]	59	59±7	0	12.1±2	2.0±0.3

The results of this analysis are demonstrated in Fig. 6, for the ortho-terphenyl viscosity data of Plazek, Bero, and Chay [43]. The optimal $T_c=-65\,°C$, is indicated by the black circles, and other T_c with correlation coefficients larger than $0.999r^2$ are shown as gray circles. Such an analysis yields the asymmetric error bars of Fig. 5, which have the expected correlation between T_c and νz that result in curved error bars. Figure 6 also shows that the scaling analysis only applies to the high viscosity data that are sufficiently close to T_c. The scaling naturally breaks down at high temperatures, where there is sufficient free volume everywhere for liquid-like motion (i.e., $n=1$).

Most of the polymers (triangles in Fig. 5) appear to be in one universality class, which Angell terms ''fragile.'' Nearly all polymers have $T_g-T_c<20\,K$ and $8<\nu z<11$. The differences in T_g-T_c are most likely related to the rather different arbitrary definitions of T_g used by different groups. We conclude that $\nu z\cong 9$ and $T_g-T_c\cong 10\,K$ for all polymers. With $z=6$, the finding that $\nu z=9$ means that $\nu=\frac{3}{2}$ for polymers. The notable exceptions are cis-polyisoprene and atactic polypropylene, which appear to have considerably larger νz exponents. One of the inorganic glasses (selenium) also appears to be in the universality class with the polymers. This is hardly surprising, since selenium is believed to be polymeric [44]. Assuming $\nu z=9$, we can rewrite Eq. (1) as

$$\tau\sim(T-T_c)^{-9} \quad \text{for polymers.} \tag{22}$$

This is tested directly in Fig. 7, which seems to provide a reasonable means to determine T_c for polymers (as the temperature at which the relaxation time diverges).

Three conclusions can be reached from Fig. 7. The high-temperature data for PVME and polybutadiene show that the scaling regime where Eq. (22) is valid is limited to within roughly 100 K of T_c. This is expected, because at high temperature there is sufficient free volume everywhere for each

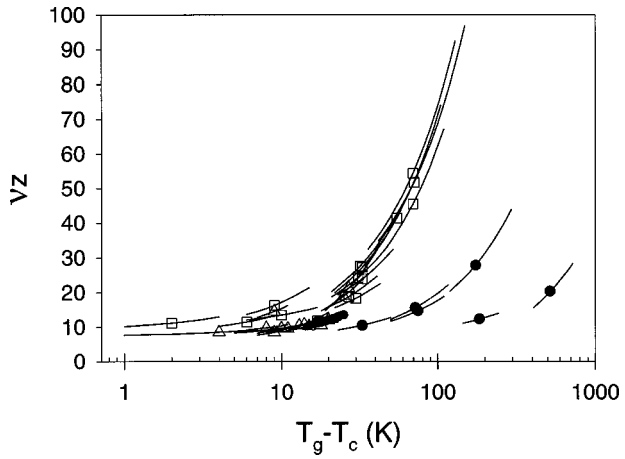

FIG. 5. Correlation of the exponent νz with $T_g - T_c$ for the glass-forming liquids listed in Table I, including flexible polymers (open triangles), organic small molecules (open squares) and inorganic glasses (filled circles). The solid curves are error bars described in the text.

particle to move independently. The size of the largest cluster decreases with temperature and eventually reaches the particle size, where the scaling picture no longer applies. All data sets used to generate Table I and Fig. 5 were truncated at high temperature when the scaling form no longer fit the data. Comparison of PVE and PVME shows that the prefactor in Eq. (22) is not universal for all polymers. Comparison of cis-PI with 1,4-PI in Fig. 7 indicate that their differences are not as large as Table I and Fig. 6 suggest. The data for cis-PI need confirmation. One can see from Fig. 7 that the data set of Plazek, Tan and O'Rourke [23] for PMMA contains the largest relaxation times (and gets closest to T_c), perhaps explaining why the Vogel form was only observed to fail for PMMA. The different T_c obtained from DS and

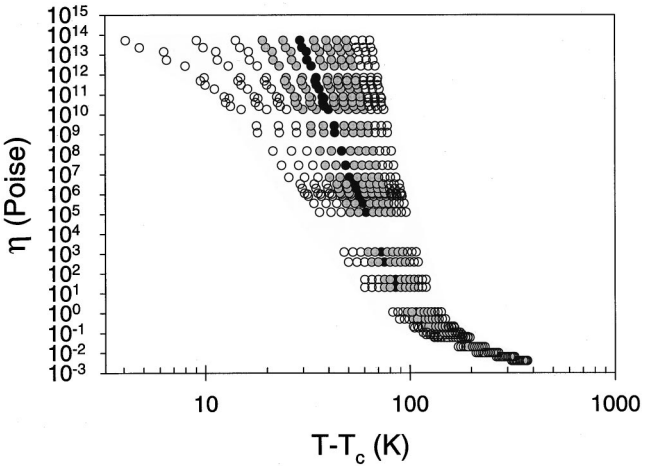

FIG. 6. Viscosity data (Ref. [42]) of Plazek *et al.* (Ref. [43]) for ortho-terphenyl, fit to Eq. (1) using, from left to right, $T_c = -40$, -45, -50, -55, -60, -65, -70, -75, -80, -85, -90, -95, and $-100\,^{\circ}\mathrm{C}$. The optimal $T_c = -65\,^{\circ}\mathrm{C}$ (black circles) has the largest correlation coefficient ($r^2 = 0.9966$), while the gray circles for $T_c = -55$, -60, -70, -75, -80, and $-85\,^{\circ}\mathrm{C}$ have correlation coefficients larger than $0.999r^2$. The temperatures with correlation coefficients smaller than this value have open circles. Only the viscosities exceeding 10^4 Poise were used for this analysis.

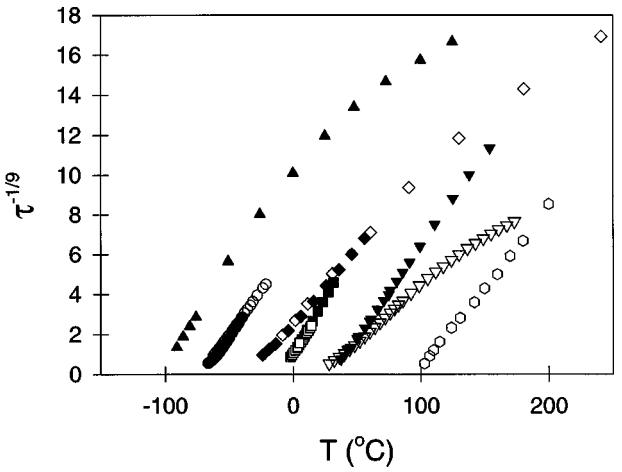

FIG. 7. Scaling plot to determine T_c for flexible polymers, assuming $\nu z = 9$, applied to PB [triangles from OS (Ref. [65])], cis-PI [filled circles from OS (Ref. [22])], 1,4-PI [open circles from DS (Ref. [60])], PVME [filled diamonds from OS (Ref. [12]), open diamonds from OS (Ref. [13])], PVE [filled squares from DS (Ref. [61]), open squares from DS (Ref. [60])], PVAc [inverted filled triangles from creep (Refs. [56] and [57]), inverted open triangles from DS (Ref. [52])], and PMMA [open hexagons from creep (Ref. [23])].

creep results on polyvinylacetate seen in Fig. 7 and Table I may possibly be the result of different tacticities of the two polymers studied.

The floppy organic small molecule glass formers (squares in Fig. 5) have much larger exponents ($13 < \nu z < 55$), and also larger fragility parameters ($9\,\mathrm{K} \leqslant T_g - T_c \leqslant 71\,\mathrm{K}$) making them stronger glasses in Angell's classification. The unphysically large values of the exponent νz, coupled with the seemingly uncontrolled errors (± 30 in νz is not uncommon) force us to question whether the scaling approach really applies to the small organic molecules, despite excellent fits of their viscosity [42] to Eq. (1). There appears to be a trend of increasing νz with an increase in $T_g - T_c$, for the small molecule organic glass-formers. These results suggest that for the organic small molecules, it is not enough to simply have a free volume of the proper size. There may be some additional energy barriers restricting motion [4,15,45], as discussed in detail below.

Angell refers to SiO_2, GeO_2, and B_2O_3 as ''strong'' glasses because the critical temperature is far below the apparent glass transition ($T_g - T_c > 100\,\mathrm{K}$). However, the trend of increasing νz as the glasses become stronger, observed for the floppy organic small molecules, does not hold for the inorganic glass-formers. B_2O_3 has the largest $\nu z = 28$ of the strong inorganic glass formers. GeO_2 has a similar $T_g - T_c$, but has $\nu z = 12$. Figure 5 and Table I demonstrate the lack of universality in both νz and $T_g - T_c$.

The nonuniversal character of glass formation is made very evident when νz from the temperature dependence of relaxation and $z = 6$ from Andrade creep are combined to determine the correlation length exponent ν (last column in Table I). Instead of being universal, this important exponent apparently varies over a wide range ($1.4 \leqslant \nu \leqslant 9$). We attempt a simple explanation of this nonuniversality amongst the nonpolymeric glass formers using material-specific energetic barriers to motion [4,15,45] in the next section.

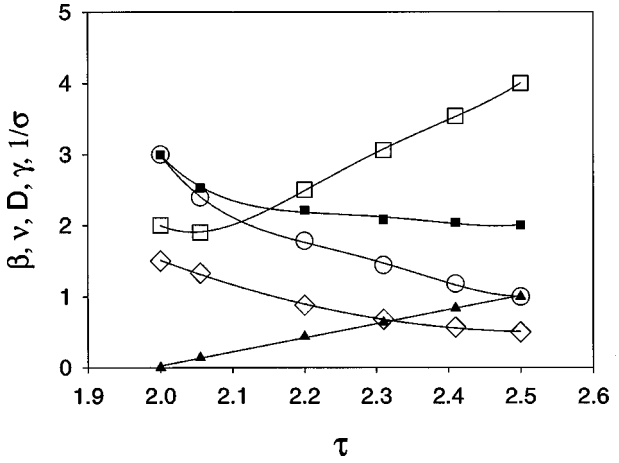

FIG. 8. Scaling exponents for glass formation ($\tau=2$), and percolation in various dimensions (Ref. [31]) ($d=2$ has $\tau=187/91=2.05$, $d=3$ has $\tau=2.2$, $d=4$ has $\tau=2.3$, $d=5$ has $\tau=2.4$, and $d=6$ has $\tau=5/2$): Order parameter exponent β (filled triangles), correlation length divergence exponent ν (open diamonds), fractal dimension D (open squares), weight-average cluster size divergence exponent γ (open circles), and largest cluster size divergence exponent $1/\sigma$ (filled squares). The curves are simply guides for the eye.

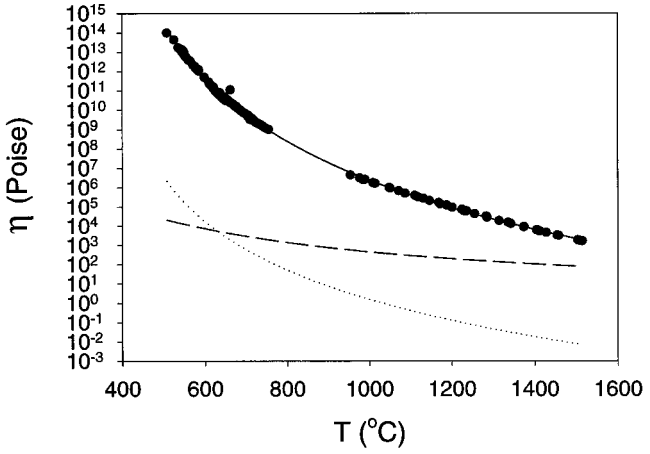

FIG. 9. Temperature dependence of viscosity for the inorganic glass-former GeO_2. Filled circles are data of Fontana and Plummer (Ref. [46]) and the solid curve is the regression fit to Eq. (23). The dashed curve is the Arrhenius part of Eq. (23) [$\exp(E/kT)$ and the dotted curve is the algebraic divergence in Eq. (23) ($[(T-T_c)/T_c]^{-9}$).

IV. DISCUSSION

For polymers, $\nu=\frac{3}{2}$ is apparently universal (obtained from the experimental findings that $\nu z=9$ and $z=6$). This exponent makes $\gamma=1/\sigma=3$. All exponents for glass formation are then smooth continuations of the exponents for percolation [31] in dimensions $d=2$, 3, 4, 5, and 6, as shown in Fig. 8. The upper critical dimension for percolation is $d=6$, meaning that in six dimensions the mean-field exponents hold (with $\tau=\frac{5}{2}$) As d is decreased, τ progressively decreases, and extrapolation beyond $\tau=187/91$ for $d=2$ percolation to $\tau=2$ for glass formation leads directly to the conclusion that $\nu=\frac{3}{2}$. This strongly suggests that there may be some utility to the scaling approach for understanding glass formation in polymers. The physics behind the exponent $\nu=\frac{3}{2}$ deserves further theoretical attention.

The nonuniversality in ν, seen for non-polymeric glass-forming liquids in Table I, strongly suggests that something is missing from the simple scaling picture described above. The scaling picture is built around an order parameter that is the fraction of all space with enough free volume for motion. Based on the successful description of polymers, with $\tau=2$ and $\nu=\frac{3}{2}$, and the fact that all the exponents in this class are logical extrapolations of the known percolation exponents (see Fig. 8), we suggest that having the requisite free volume is a necessary condition, but not a sufficient condition for motion in nonpolymeric glass-forming liquids. Specifically, we make the ansatz that the above scaling description with $\tau=2$ and $\nu=\frac{3}{2}$ properly describes the disappearance of free volume as temperature is lowered in *every* glass-forming liquid, but there are material-specific energetic barriers to motion [4,15,45], described by an activation energy E. Such considerations lead to the following simple expression for the temperature dependence of the relaxation time (or viscosity) of all glass-forming liquids,

$$\tau\sim\eta\sim\left(\frac{T-T_c}{T_c}\right)^{-9}\exp\left(\frac{E}{kT}\right). \tag{23}$$

Two material-specific parameters thus describe the temperature dependence, a critical temperature T_c and an activation energy E. Equation (23) has the same number of parameters are the empirical Vogel relation [Eq. (4)]. We demonstrate the ability of Eq. (23) to describe data using the viscosity data for the strong inorganic glass former [46] GeO_2 in Fig. 9. The resulting fit parameters are $T_c=379\,^\circ\mathrm{C}$ and $E=65\,\mathrm{kJ/mol}$, and the fit is shown as the solid curve. The critical temperature is comparable to that obtained previously (see Table I). The temperature dependence of the Arrhenius part of Eq. (23) [i.e., $\exp(E/kT)$] is shown as the dashed curve in Fig. 9, while the algebraic divergence part $\{[(T-T_c)/T_c]^{-9}\}$ is shown as the dotted line. Although the Arrhenius part does weakly decrease with temperature, *the algebraic divergence dominates the temperature dependence of viscosity*, even for this strong glass. The Arrhenius temperature dependence simply allows the algebraic divergence to adopt a universal exponent of $-\nu z=-9$.

The full results of fitting the nonpolymeric viscosity and relaxation time data to Eq. (23) are presented in Table II. With the exception of SiO_2, for which more data are clearly needed, the critical temperature resulting from a fit to Eq. (23) is larger than for the simple scaling fit with $E=0$ and adjustable νz. The critical temperatures from different experiments agree very well for all glass-forming liquids (see Table II entries for ortho-terphenyl, salol, and propylene carbonate). The activation energies from dielectric spectroscopy are consistently smaller than those from viscosity measurements, accounting for the different temperature dependences from the two methods. Several of the glass-forming liquids have T_c very close to T_g, and the finding that T_c is actually above T_g for $[KNO_3]_{40}[Ca(NO_3)_2]_{60}$ probably reflects an error in the experimental estimation of the glass transition. Whenever available, we used glass transition data from origi-

TABLE II. Critical temperatures and activation energies for nonpolymeric glass-forming liquids fit to Eq. (23).

Material	method	T_g (°C)	T_c (°C)	$T_g - T_c$ (K)	E (kJ/mol)
SiO_2	viscosity [46,48]	1173	440±100	730	230
GeO_2	viscosity [46]	545	379±4	166	65
B_2O_3	viscosity [49]	275	218±6	57	75
$Pd_{48}Ni_{32}P_{20}$	kinetics [50]	292	239±2	53	92
$Pt_{45}Ni_{56}P_{25}$	kinetics [50]	209	156±2	53	96
Aroclor 1248	creep [43]	−50	−95±4	45	190
6-phenyl ether	creep [43]	−25	−53±7	28	220
$Pd_{77.5}Cu_6Si_{16.5}$	kinetics [50]	340	312±1	28	42
ortho-terphenyl	DS [52,54]	−29	−46±1	17	120
ortho-terphenyl	creep [43]	−32	−50±2	18	160
ortho-terphenyl	viscosity [51]	−33	−49±1	16	160
kresolphtalein-dimethylether	DS [55,52]	38	21±1	17	105
phenolphtalein-dimethylether	DS [55,52]	21	5±1	16	120
salol	DS [52,53]	−53	−70±1	17	110
salol	viscosity [51]	−60	−74±3	14	120
1-propanol	DS [52,54]	−168	−182±1	14	8
α-phenyl-*o*-cresol	viscosity [51]	−63	−72±1	9	80
glycerol	DS [62]	−93	−98±1	5	28
propylene carbonate	viscosity [64]	−119	−124±1	5	54
propylene carbonate	DS [52,53]	−116	−121±1	5	17
2-methyltetrahydrofuran	DS [66,52]	−182	−183±1	1	8
$[KNO_3]_{60}[Ca(NO_3)_2]_{40}$	viscosity [67]	59	64±1	−5	45

nal references [67] but more modern methods suggest that $T_g = 66$ °C for $[KNO_3]_{60}[CaNO_3]_{40}$ [68] making $T_g - T_c = 3$ K in Table II.

V. CONCLUSIONS

We present compelling experimental evidence that the scaling form [Eq. (1) and ultimately Eq. (23)] for the temperature dependence of relaxation time in glass-forming liquids is superior to the empirical Vogel form [Eq. (4)]. Indeed, Eq. (23) can describe the temperature dependence of relaxation in all glass-forming liquids with two material parameters: the critical temperature T_c and the activation energy E. Either form can describe the experimental relaxation time (or viscosity) in the range $T_g < T < T_g + 100$ K. However, relaxation monitored by different techniques consistently give identical critical temperatures, while the Vogel temperatures can differ by as much as 25 K, and only have an experimental uncertainty of ±3 K. Furthermore, the critical temperature is not as far below T_g as the Vogel temperature. To unambiguously test whether either form is correct, relaxation times must be measured for *equilibrium* glasses between T_c and T_g. The difficulty with these measurements is that the approach to equilibrium can be very slow. For polymers, one typically needs to wait 100 h, 5 K below T_g, to age the glass into the equilibrium state [47]. However, these experiments will allow measurements closer to T_c that should easily distinguish between the scaling and Vogel forms.

Using the simple idea that free volume diffuses randomly, we have constructed a scaling description of glass formation. Random diffusion of free volume creates random-walk clusters of cooperatively rearranged particles with fractal dimension $D = 2$. As T_c is approached from above, progressively larger clusters are formed because more time is needed for the entire sample to experience motion. We calculate the distribution of cooperatively rearranging regions, and find that it is described by a power law with exponent $\tau = 2$. However, our model is incomplete because we have not calculated the exponents that describe the divergences of the largest cooperatively rearranging region and its relaxation time as the critical temperature is approached from above. Future theoretical work should focus on calculating these exponents.

In the absence of theory, we turned to experiments on glass-forming liquids to evaluate these exponents. The dynamic exponent $z = 6$ was determined from the empirical Andrade creep observed for all glass-forming materials. With $z = 6$, $\tau = 2$, and $D = 2$ our scaling model predicts the distribution of segmental relaxation times, which is in reasonable agreement with experiments. Experimental data for the temperature dependence of relaxation time (or viscosity) determined the exponent product νz. We are encouraged by the observation that all polymers appear to be in a single-universality class and that the model applies very well for all polymers, with $\nu z = 9$, suggesting that $\nu = \frac{3}{2}$. This exponent is precisely what is expected from a simple extrapolation of $\nu(\tau)$ using percolation models in various dimensionalities. Therefore, we expect $\nu = \frac{3}{2}$ is universal for all glass-forming liquids.

Nonpolymeric glass-forming liquids have much stronger divergences of viscosity than polymers, which suggests that the creation of the requisite free volume is not a sufficient condition for motion in nonpolymeric glass formers. Excellent fits of the temperature dependence of viscosity (or relax-

ation time) are obtained for these materials using $\nu=\frac{3}{2}$ and $z=6$ (i.e., $\nu z=9$), coupled with a thermally activated process [Eq. (23)]. The stronger glasses have substantial activation energies, but the algebraic divergence from the scaling theory dominates the temperature dependence of relaxation processes. A theoretical explanation of why the activation energy is zero (or very small) for polymers and substantial for strong glass formers is clearly needed. Replica methods appear promising for such calculations [69,70].

ACKNOWLEDGMENTS

Financial support from the National Science Foundation through Grant No. DMR-9977928 is gratefully acknowledged. We thank J. F. Douglas, G. Fytas, S. C. Glotzer, A. Halperin, S. Y. Kamath, S. K. Kumar, M. Rubinstein, and particularly C. P. Lusignan for discussions. We also thank G. Floudas, S. C. Glotzer, S. R. Nagel, J. A. Pathak, D. J. Plazek, and C. M. Roland for supplying data.

[1] M. C. Shen and A. V. Tobolsky, Adv. Chem. Ser. **48**, 27 (1965).
[2] J.-L. Barrat and M. L. Klein, Annu. Rev. Phys. Chem. **42**, 23 (1991).
[3] C. A. Angell, Science **267**, 1924 (1995).
[4] S. Alexander, Phys. Rep. **296**, 65 (1998).
[5] H. E. Stanley, *Introduction to Phase Transitions and Critical Phenomena* (Oxford University Press, Oxford, 1971).
[6] P. H. Poole, C. Donati, and S. C. Glotzer, Physica A **261**, 51 (1998).
[7] C. Bennemann, C. Donati, J. Baschnagel, and S. C. Glotzer, Nature (London) **399**, 246 (1999).
[8] J. Souletie, J. Phys. (France) **51**, 883 (1990).
[9] F. Mezei, Ber. Bunsenges. Phys. Chem. **95**, 1118 (1991).
[10] G. Adam and J. H. Gibbs, J. Chem. Phys. **43**, 139 (1965).
[11] P. C. Hohenberg and B. I. Halperin, Rev. Mod. Phys. **49**, 435 (1977).
[12] J. A. Pathak, R. H. Colby, G. Floudas, and R. Jerome, Macromolecules **32**, 2553 (1999).
[13] R. M. Kannan and T. P. Lodge, Macromolecules **30**, 3694 (1997).
[14] H. Vogel, Phys. Z. **22**, 645 (1921).
[15] J. P. Sethna, J. D. Shore, and M. Huang, Phys. Rev. B **44**, 4943 (1991).
[16] G. Floudas, G. Fytas, and E. W. Fischer, Macromolecules **24**, 1955 (1991).
[17] D. J. Plazek, X. D. Zheng, and K. L. Ngai, Macromolecules **25**, 4920 (1992).
[18] D. J. Plazek, E. Schlosser, A. Schoenhals, and K. L. Ngai, J. Chem. Phys. **98**, 6488 (1993).
[19] A. Schonhals, Macromolecules **26**, 1309 (1993).
[20] D. J. Plazek *et al.*, Colloid Polym. Sci. **272**, 1430 (1994).
[21] P. G. Santangelo, K. L. Ngai, and C. M. Roland, Macromolecules **29**, 3651 (1996).
[22] P. G. Santangelo and C. M. Roland, Macromolecules **31**, 3715 (1998).
[23] D. J. Plazek, V. Tan, and V. M. O'Rourke, Rheol. Acta **13**, 367 (1974).
[24] J. D. Ferry, *Viscoelastic Properties of Polymers*, 3rd ed. (Wiley, New York, 1980), Chap. 11, pp. 277–279.
[25] J. Baschnagel, M. Wolfgardt, W. Paul, and K. Binder, J. Res. Natl. Inst. Stand. Technol. **102**, 159 (1997).
[26] W. Gotze and L. Sjogren, Rep. Prog. Phys. **55**, 241 (1992).
[27] H. Sillescu, J. Non-Cryst. Solids **243**, 81 (1999).
[28] M. H. Cohen and D. Turnbull, J. Chem. Phys. **31**, 1164 (1959).
[29] G. S. Grest and M. H. Cohen, Adv. Chem. Phys. **48**, 455 (1981).
[30] C. Donati *et al.*, Phys. Rev. Lett. **80**, 2338 (1998).
[31] D. Stauffer and A. Aharony, *Introduction to Percolation Theory*, 2nd ed. (Taylor and Francis, London, 1992).
[32] C. P. Lusignan, 1998 (private communication).
[33] S. C. Glotzer and C. Donati, J. Phys.: Condens. Matter **11**, A285 (1999).
[34] C. Donati, S. C. Glotzer, P. H. Poole, W. Kob, and S. J. Plimpton, Phys. Rev. E **60**, 3107 (1999).
[35] To inhibit crystallization, the simulation used $\frac{4}{5}$ type-*A* particles and $\frac{1}{5}$ type-*B* particles, with different sizes and interaction energies.
[36] R. H. Colby, J. R. Gillmor, and M. Rubinstein, Phys. Rev. E **48**, 3712 (1993).
[37] C. P. Lusignan, T. H. Mourey, J. C. Wilson, and R. H. Colby, Phys. Rev. E **52**, 6271 (1995).
[38] E. N. da C. Andrade, Proc. R. Soc. London, Ser. A **84**, 1 (1910).
[39] J. D. Ferry, *Viscoelastic Properties of Polymers*, 3rd ed. (Wiley, New York, 1980), Chap. 13, pp. 392–94.
[40] C. A. Bero, Ph.D. thesis, University of Pittsburgh, 1994 (unpublished).
[41] S. Havriliak and S. J. Havriliak, *Dielectric and Mechanical Relaxation in Materials* (Hanser, 1997).
[42] Many of the nonpolymeric glasses only have viscosity data, and we assume the relaxation time is proportional to the viscosity.
[43] D. J. Plazek, C. A. Bero, and I. C. Chay, J. Non-Cryst. Solids **172–174**, 181 (1994).
[44] A. Eisenberg and A. V. Tobolsky, J. Polym. Sci. **61**, 483 (1962).
[45] L. Angelani, G. Parisi, G. Ruocco, and G. Viliani, Phys. Rev. Lett. **81**, 4648 (1998).
[46] E. H. Fontana and W. A. Plummer, Phys. Chem. Glasses **7**, 139 (1966).
[47] J. M. Hutchinson, Prog. Polym. Sci. **20**, 703 (1995).
[48] R. Bruckner, J. Non-Cryst. Solids **5**, 177 (1971).
[49] P. B. Macedo and A. Napolitano, J. Chem. Phys. **49**, 1887 (1968).
[50] H. S. Chen, J. Non-Cryst. Solids **27**, 257 (1978).
[51] W. T. Laughlin and D. R. Uhlmann, J. Phys. Chem. **76**, 2317 (1972).
[52] F. Stickel, Ph.D. thesis, Universitat Mainz, 1995 (unpublished).
[53] F. Stickel, E. W. Fischer, and R. Richert, J. Chem. Phys. **104**, 2043 (1996).
[54] C. Hansen, F. Stickel, T. Berger, R. Richert, and E. W. Fischer, J. Chem. Phys. **107**, 1086 (1997).
[55] F. Stickel, F. Kremer, and E. W. Fischer, Physica A **201**, 318 (1993).
[56] D. J. Plazek, Polym. J. (Singapore) **12**, 43 (1980).

[57] D. J. Plazek, J. Polym. Sci., Part B: Polym. Phys. **20**, 729 (1982).
[58] K. Ueberreiter and H.-J. Orthmann, Kolloid-Z. **123**, 84 (1951).
[59] G. Faivre and J.-L. Gardissat, Macromolecules **19**, 1988 (1986).
[60] S. Kamath *et al.*, J. Chem. Phys. **111**, 6121 (1999).
[61] A. Alegra, J. Colmenero, K. L. Ngai, and C. M. Roland, Macromolecules **27**, 4486 (1994).
[62] N. Menon *et al.*, J. Non-Cryst. Solids **141**, 61 (1992).
[63] D. L. Plazek and D. J. Plazek, Macromolecules **16**, 1469 (1983).
[64] A. Bondeau and J. Huck, J. Phys. (France) **46**, 1717 (1985).
[65] R. H. Colby, L. J. Fetters, and W. W. Graessley, Macromolecules **20**, 2226 (1987).
[66] R. Richert, F. Stickel, R. S. Fee, and M. Maroncelli, Chem. Phys. Lett. **229**, 302 (1994).
[67] R. Weiler, S. Blaser, and P. B. Macedo, J. Phys. Chem. **73**, 4147 (1969).
[68] D. L. Sidebottom and C. M. Sorensen, J. Chem. Phys. **91**, 7153 (1989).
[69] M. Mézard and G. Parisi, Phys. Rev. Lett. **82**, 747 (1999).
[70] M. Mézard and G. Parisi, J. Chem. Phys. **111**, 1076 (1999).